Hindawi
Journal of Electrical and Computer Engineering
Volume 2022, Article ID 3615307, 15 pages
https://doi.org/10.1155/2022/3615307

Research Article

Supervisory Control Scheme of a Wind Farm Connected to a Hybrid Microgrid

Mustapha Benghanem,[1] Abdulrahmane AlKassem,[2] Abdelhaq Amar Bensaber,[1] and Azeddine Draou[2]

[1]*University of Science and Technology of Oran, College of Electrical Engineering, Department of Automatic Control, Oran, Algeria*
[2]*Department of Electrical Engineering, College of Engineering, Islamic University of Madinah, Madinah 42361, Saudi Arabia*

Correspondence should be addressed to Azeddine Draou; az_draou@iu.edu.sa

Received 23 May 2022; Revised 18 August 2022; Accepted 2 September 2022; Published 3 October 2022

Academic Editor: Bhargav Appasani

Nowadays, the generation of wind power combined with a battery energy storage system offers a viable solution for electricity supply to isolated areas with no access to the grid. However, the speed of the wind is unpredictable and the inherent nonlinearities of the wind turbine and generator system cause fluctuations in the voltage, power, and frequency. This paper proposes a new three-layered control technique applied to a wind farm that uses doubly-fed induction generators (DFIGs) connected to a remote hybrid microgrid. The first layer provides local control to each DFIG wind turbine based on a nonlinear and robust control strategy. The second layer coordinates and controls the flow of power between the turbine and the storage system to make sure that load demand is being satisfied and the desired limits of the state of charge are respected. Finally, and in the third layer, we implement a supervisory controller that will be responsible for the generation of the references for the active power as per the load demand. The proposed off-grid wind power system and battery storage and its three-layer hierarchical control scheme are simulated under MATLAB/Simulink environment and tested under various load and speed profiles. Through the numerous test data obtained, it has been shown that the control strategy under study is robust and effective.

1. Introduction

Many rural communities across the globe, especially in developing countries, have limited access to the electricity grid due to the high cost of grid extension and rough topography. Solar and wind energy sources can offer a viable alternative solution for electricity generation. Renewable energy sources have many advantages like reduced environmental impact, conservation of energy, and inexhaustible sources [1, 2]. Standalone energy systems have turned out to be the most promising ones for such remote areas [3–5]. Moreover, wind energy resource has proven to be more adequate for sustainable power delivery with reduced storage capacity [6, 7].

However, in a microgrid system, battery energy storage system is inserted for a balance of energy demand, and an energy management strategy is used not only to control the charging state of the battery for a longer lifetime but also to eliminate the power fluctuation for a better quality of power to the load.

Several techniques have been used in the literature to provide good power management, such as classical PI and PID controllers [2, 5], and intelligent controllers using uzzy logic [8–10].

The doubly-fed induction generator-based wind turbines have, in recent years, become very popular due to their numerous advantages such as operation with variable speed and constant frequency, MPPT capability, and power control decoupling [11]. Recently, to improve the quality of power of wind energy systems, numerous control techniques including vector control (VC) approaches have been proposed; however, under parameter variations, model uncertainties, and disturbance, the VC strategy leads to low and unrobust performances [12].

To bypass these problems, new robust techniques for the control of the DFIG such as Sliding Mode Control (SMC), intelligent and adaptive control [13–15], a new Sliding Mode Control Based on High Order (HOSMC) [13–19], and Backstepping [20–22] have been, recently, used.

SMC is an effective robust control approach for parameter variations; however, it has some drawbacks such as the chattering phenomenon that may cause performance degradation and may lead to excessive frequency oscillations [23, 24]. To overcome these drawbacks, a modified SMC [16, 25, 26] is based on an approximation of a saturation function with high gain. In this research work, a technique named Second-Order Sliding Mode Control (SOSMC) is used due to its many advantages such as robustness, good tracking under uncertainties, suppression of mechanical stresses and chattering, and ease of implementation.

In this paper, we propose a three-layered power control scheme for a DFIG-based Wind Farm, where each Wind Turbine Generator (WTG) is equipped with a battery. In the first layer and to attain maximum performance, SOSMC is used.

In the second layer, we implemented a controller based on Fuzzy Logic. This controller will not only manage and optimize the power flow for different modes but also maintain the state of charge at an acceptable level for any islanded community using a wind-battery standalone system.

In the third layer, the power references used in the second layer are generated. Finally, some simulation tests are carried out based on the MatLab environment to test the usefulness of the proposed control strategy.

2. Description and Modeling of the Wind Energy System and Battery

The system considered in this study as depicted in Figure 1 shows a block diagram of the system under consideration. The hybrid power system consists of a wind farm, battery bank, and Power Electronics converters connected to the proposed controller.

2.1. Wind Turbine Model and MPPT Control. The power contained in a mass of air crossing a surface area A_1 at a wind speed V_v is given by [27]

$$P_v = \frac{1}{2}\rho A_1 V_v^3, \tag{1}$$

where ρ represents the density of air.

The power recovered by the wind turbine is as follows:

$$P_t = \frac{1}{2}\rho\pi R^2 V_v^3 C_p, \tag{2}$$

where R represents the blades radius and C_p represents the coefficient of power [16].

The speed ratio λ is given by

$$\lambda = \frac{R\Omega_t}{V_v}, \tag{3}$$

where Ω_t denotes the rotor angular speed.

The rotor mechanical torque is expressed by

$$T_t = \frac{P_t}{\Omega_t} = \frac{\pi}{2\lambda}\rho R^3 v^2 C_p. \tag{4}$$

2.2. MPPT System. Figure 2 shows the maximum power efficiency of the wind turbine, where the optimal power curve is obtained for the MPP of each power curve. The control system will have to follow the tracking characteristic curve of the wind turbine.

Direct speed controller (DSC) which is used as a speed reference [13, 17] can be obtained from the optimal turbine speed at different wind speed values. Thus, the turbine rotational speed is controlled, and the mechanical power reaches the maximum value for each operating point by the regulator.

The reference used for the rotational speed is given by

$$\Omega_t^* = \frac{\left(\lambda_{\text{opt}} v\right)}{R}. \tag{5}$$

Thus,

$$\Omega_m^* = G\Omega_t^*. \tag{6}$$

The reference for the active power is defined as

$$P_{s\_\text{ref}} = C_{\text{cem\_ref}}\Omega_m. \tag{7}$$

2.3. Modeling of the Doubly-Fed Induction Generator (DFIG). The use of the DFIG is preferred as it may work in both sub and super synchronous modes. Using Park transformation, the electrical model of the machine may be obtained by the following equations [13, 14, 16]:

$$\begin{cases} V_{qs} = R_s I_{qs} + \dfrac{d\phi_{qs}}{dt} - \omega_s \phi_{ds}, \\ V_{ds} = R_s I_{ds} + \dfrac{d\phi_{ds}}{dt} - \omega_s \phi_{qs}, \\ V_{dr} = R_s I_{dr} + \dfrac{d\phi_{dr}}{dt} - \omega_s \phi_{qr}, \\ V_{qr} = R_s I_{qr} + \dfrac{d\phi_{qr}}{dt} - \omega_s \phi_{dr}. \end{cases} \tag{8}$$

2.4. Modeling of the Battery. The battery model may be represented as an equivalent circuit of the open circuit source voltage V with a series an internal resistance R as shown in Figure 3.

Then, the battery output voltage may be given as follows:

$$V_{\text{bat}} = V - I_{\text{bat}}, \tag{9}$$

where V_{bat} and I_{bat} depend on various parameters such as the variations of temperature and internal resistance.

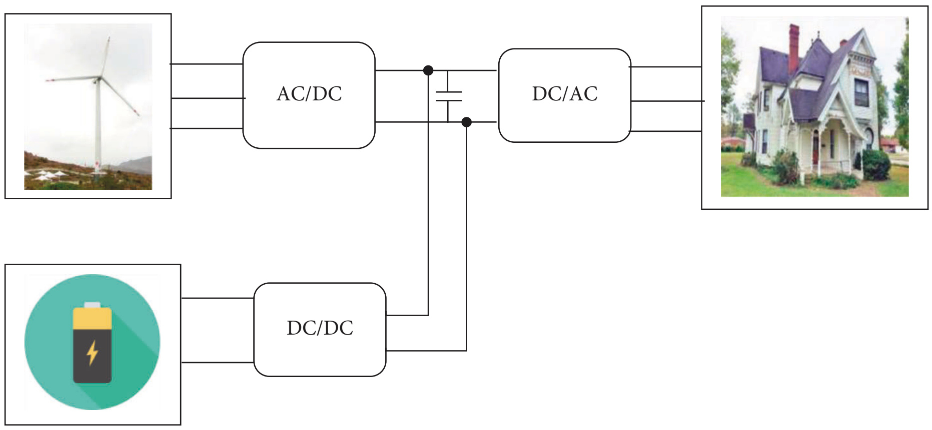

Figure 1: Configuration of the standalone hybrid energy system.

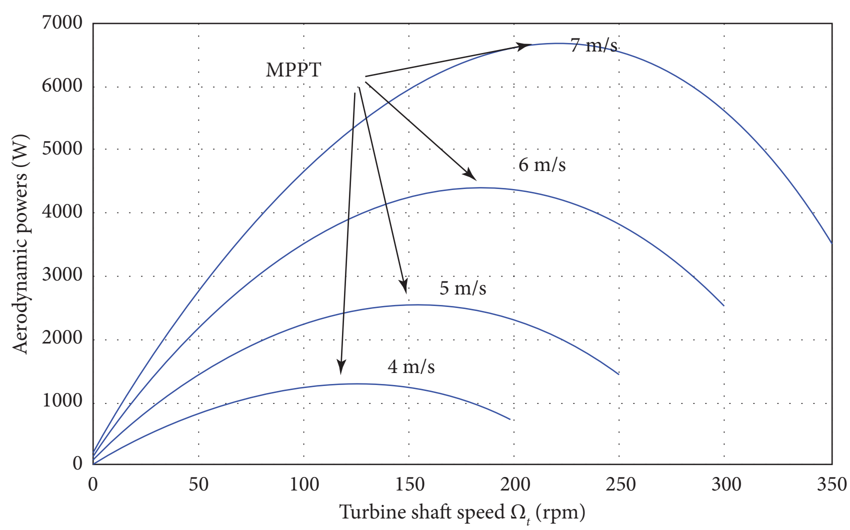

Figure 2: Maximum power efficiency of the wind turbine.

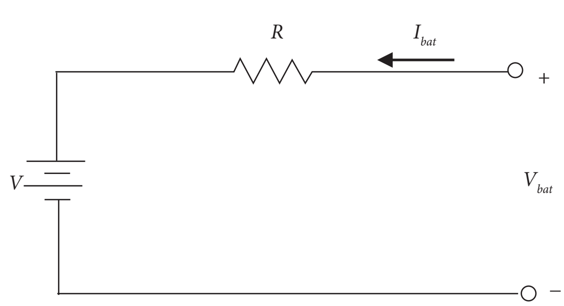

Figure 3: Model of the battery.

The SOC, during the charge and discharge process, can be defined in terms of time (t) as

$$SOC(t) = \begin{cases} SOC(t-\Delta t) + P_{\mathrm{bat}} \dfrac{\eta_{ch}}{C_n V_{dc}} \Delta t, \\ \\ SOC(t-\Delta t) + P_{\mathrm{bat}} \dfrac{1}{\eta_{\mathrm{dis}} C_n V_{dc}} \Delta t, \end{cases} \quad (10)$$

in which Δt represents the time step. P_{bat} is the power of the battery. C_n is the nominal value of the battery capacity. η_{ch} and η_{dis} are the efficiencies of the battery when the process of charge and discharge occurs. And V_{dc} is the nominal value of the DC bus voltage.

3. Power Management and Control of the Wind Energy System

In this paper, we propose a power control technique based on three layers scheme as shown in Figure 4 and may be described as follows:

(i) Wind farm supervisory control which generates the references for the active power component based on power demand

(ii) Wind turbine control which provides the local control for each DFIG wind turbine based on a nonlinear and robust control strategy

(iii) Power management which will coordinate and control the flow of power between the turbine and the storage system to make sure that load demand is

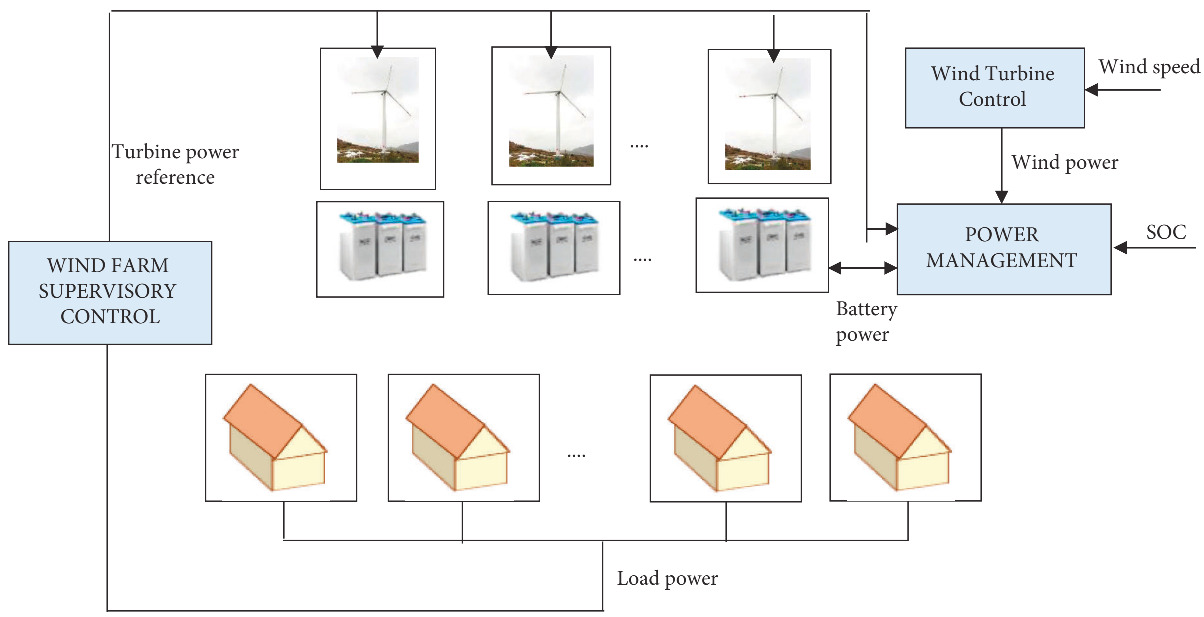

Figure 4: Proposed power management and control system.

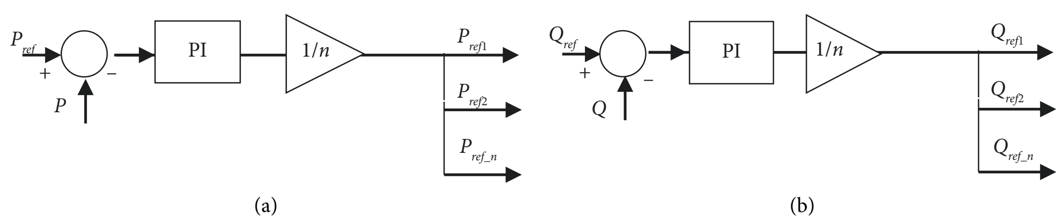

Figure 5: Proposed control scheme for the wind farm.

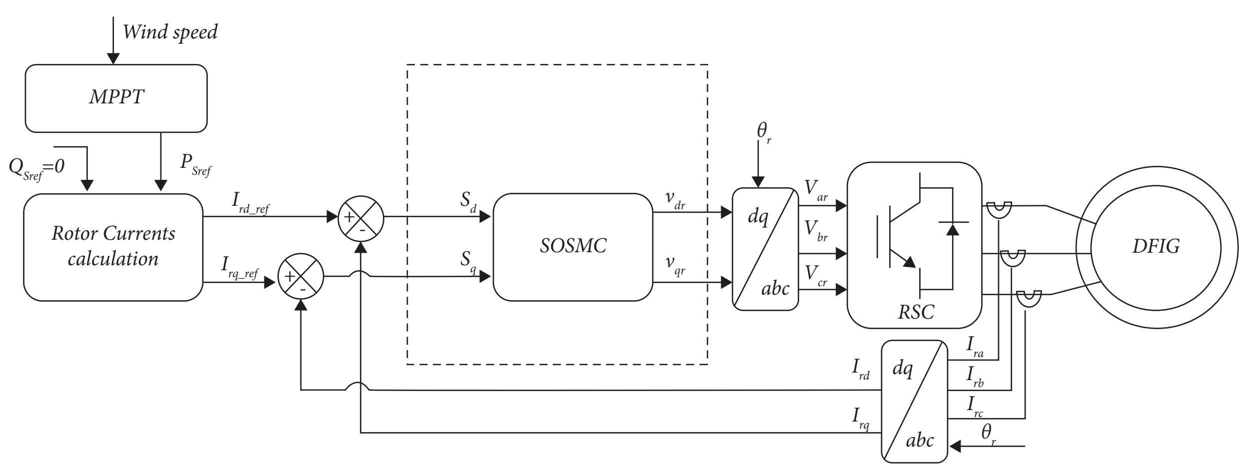

Figure 6: DFIG-based wind turbine system.

being satisfied and the desired limits of the state of charge are respected

3.1. Supervisory Control Scheme of the Wind Farm System. The objective of the wind farm supervisory controller (WFSC) is to generate the power references (Active and Reactive) for each of the wind turbines, based on the power for both directions [2, 7, 28]. This is shown in Figure 5.

3.2. Control Scheme of the Wind Turbine. The control scheme of the wind turbine that will use the generated references of the power obtained from the supervisory

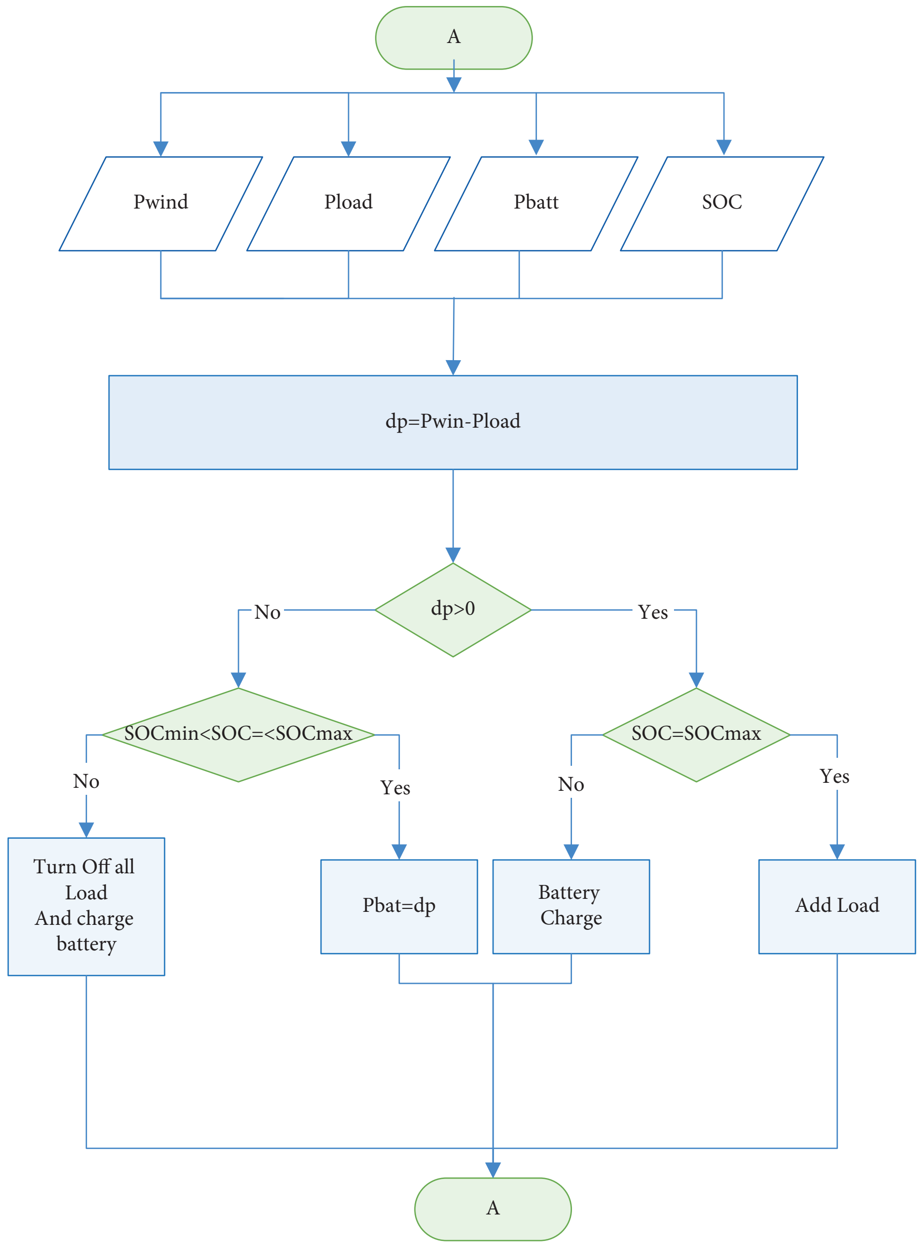

FIGURE 7: Power management flow chart.

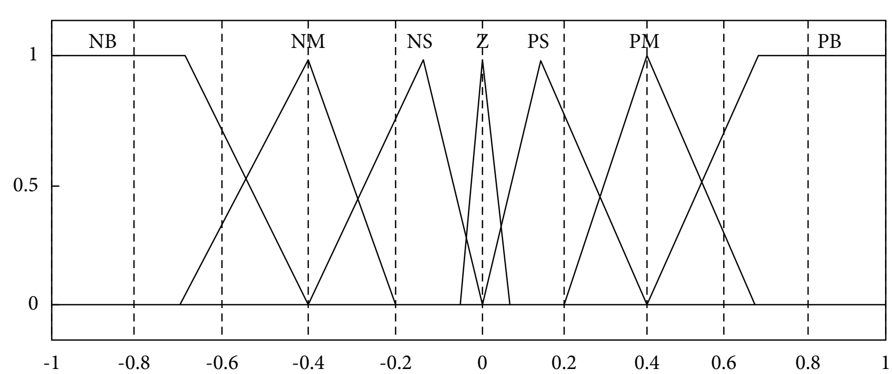

FIGURE 8: Input d_P.

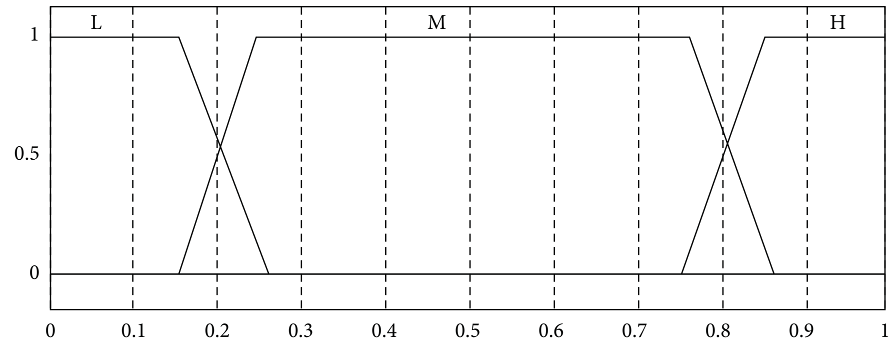

Figure 9: Input SOC.

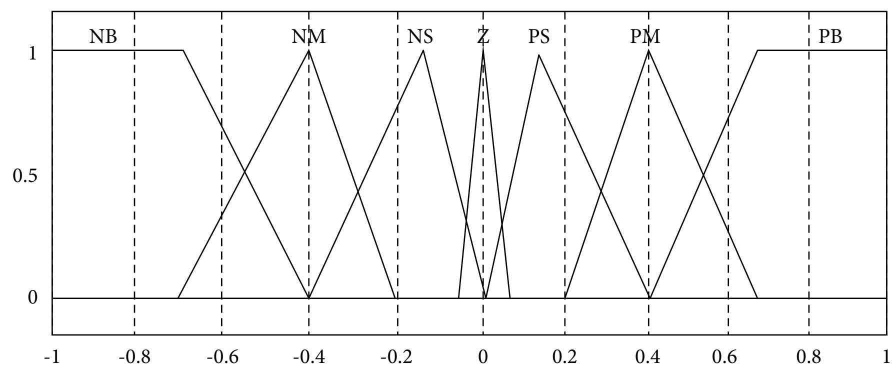

Figure 10: Output d_D.

Table 1: Fuzzy logic rules.

SOC	dP						
	PB	PM	PS	Z	NS	NM	NM
L	NB	NM	NS	Z	Z	Z	Z
M	NB	NM	NS	Z	PS	PM	PB
H	Z	Z	Z	Z	PS	PM	PB

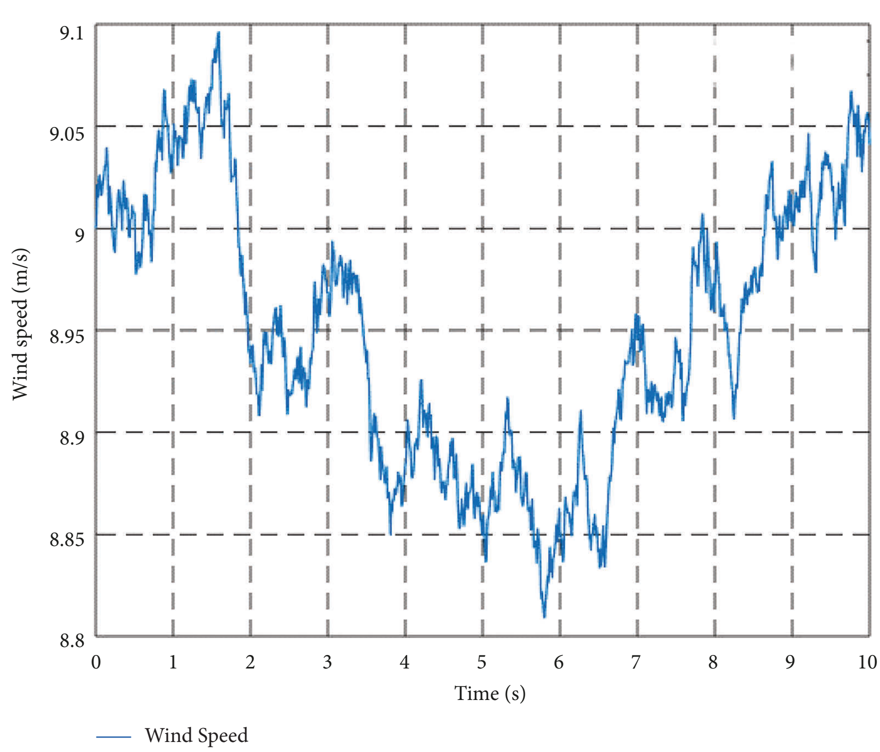

Figure 11: Wind speed profile.

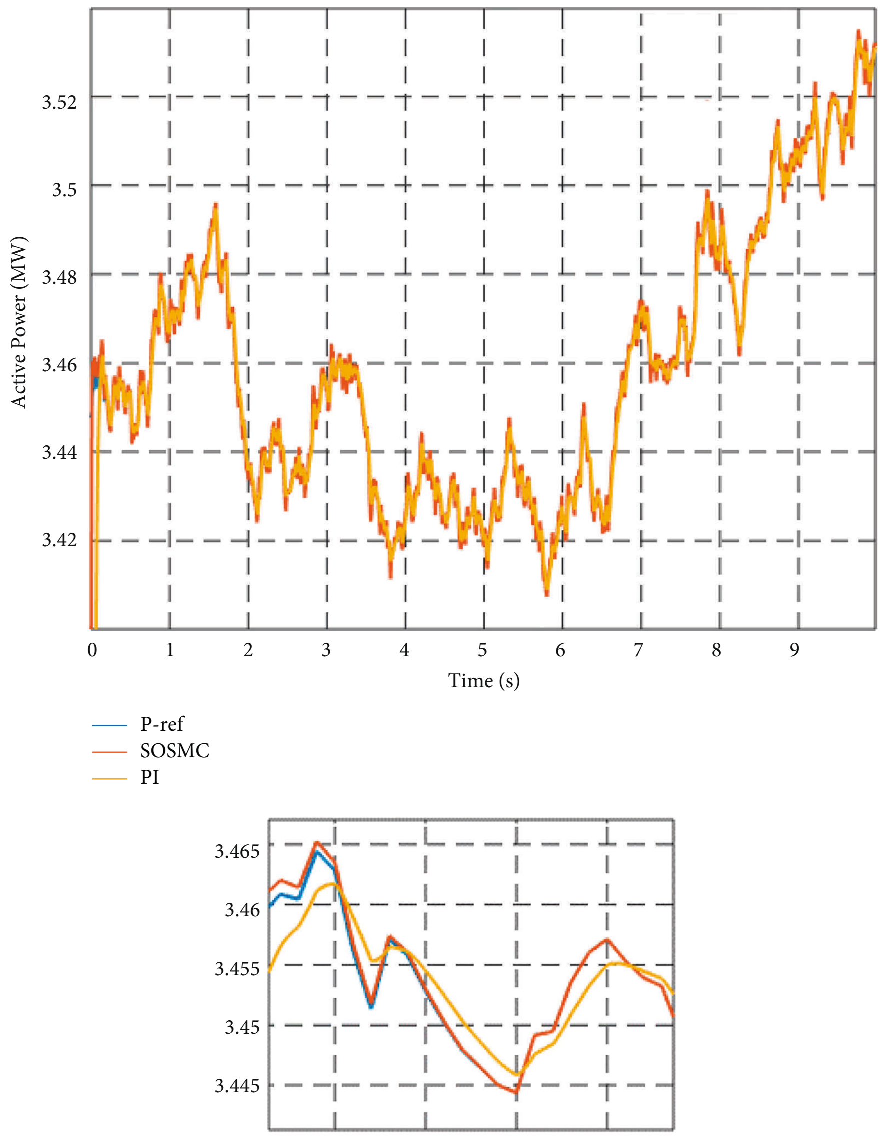

Figure 12: Active power.

controller will be analyzed according to the model shown in Figure 6.

The PID controllers although very popular and widely used in industry exhibit poor tracking performance under parameter variations and load disturbance. Although sliding mode is a viable nonlinear control scheme, its main drawback lies in the phenomenon of chattering which overheats and triggers high-frequency dynamics [15, 29].

SOSMC is another viable scheme [18] and is based on the sliding mode control approach with higher-order time derivatives. It will not only decrease the chattering phenomenon and avoid powerful mechanical efforts but will also maintain the good features of the sliding mode control [15, 18, 30].

The switching functions are defined as follows:

$$\begin{cases} S_P = e_P + c_P \int e_P dt, \\ S_Q = e_Q + c_Q \int e_Q dt. \end{cases} \quad (11)$$

The constant and positive terms c_P and c_Q are used to eliminate the steady-state errors [15, 19]. The voltage applied is given by the following equation:

$$\begin{cases} V_{dr} = V_{dreq} + V_{drn}, \\ V_{qr} = V_{qreq} + V_{qrn}. \end{cases} \quad (12)$$

The switching control V_{drn} and V_{qrn} will allow the system to reach the sliding surface whereas the equivalent control terms V_{qreq} and V_{dreq} are used to force the system to accelerate the response and move along the sliding manifold

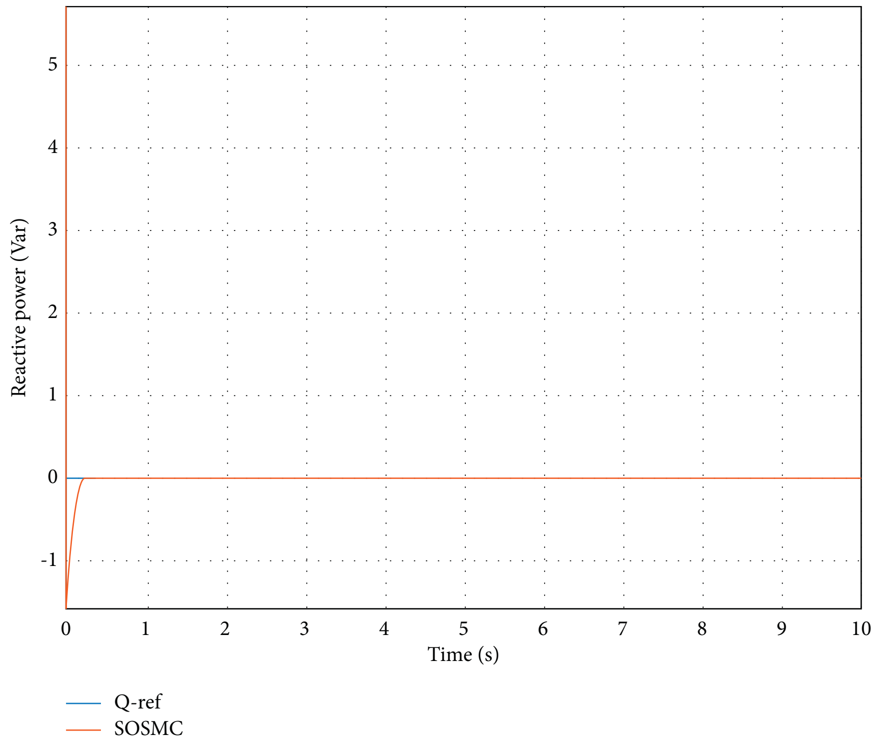

Figure 13: Reactive power.

with reduced steady-state errors [20]. The equivalent control terms are derived by letting

$$\dot{S}_P = \dot{S}_Q = 0. \tag{13}$$

The applied rotor voltages are given as follows:

$$\begin{cases} V_{qreq} = -\dfrac{L_s L_r \sigma}{MV_s}\left(\dot{P}_{s\_\text{ref}} + c_P\left(P_{s\_\text{ref}} - P_s\right)\right) + R_r I_{qr} - g w_s L_r \sigma I_{dr} - g\dfrac{MV_s}{L_s}, \\ V_{dreq} = -\dfrac{L_s L_r \sigma}{MV_s}\left(\dot{Q}_{s\_\text{ref}} + c_P\left(Q_{s\_\text{ref}} - Q_s\right)\right) + R_r I_{dr} - g w_s L_r \sigma I_{qr}. \end{cases} \tag{14}$$

Thus,

$$\begin{cases} V_{drn} = y_1 + B_1\left|e_P\right|^{\frac{1}{2}}\text{sign}\left(e_Q\right) \quad \dot{y}_1 = B_2\text{sign}\left(e_Q\right), \\ V_{qrn} = y_2 - B_3\left|e_P\right|^{\frac{1}{2}}\text{sign}\left(e_P\right) \quad \dot{y}_2 = -B_4\text{sign}\left(e_P\right), \end{cases} \tag{15}$$

where the values B_1, B_2, B_3, and B_4 are just constants.

3.3. Battery Power Management Strategy. Since the nature of renewable resources is intermittent, storage systems have become necessary in the hybrid system. Usually, batteries are used to store the excess generated power and later, if necessary, use it to supply the load [6, 31]. Moreover, a power electronic bidirectional converter is always needed for the process of charging and discharging the battery in case of power deficit or surplus [2, 7].

A controller based on fuzzy logic (FL) is implemented for the battery charge/discharge and described in this paper. The FL controller will generate for each fuzzy set in the membership function a degree of membership after obtaining the inputs, and then it will evaluate the fuzzy set memberships and decide which rules would be used before being converted into a signal as an output control [32, 33].

The controller comprises two inputs, namely, the difference between the required load power and the generated wind power (dP) as well as the SOC and one output related to the reference of battery power.

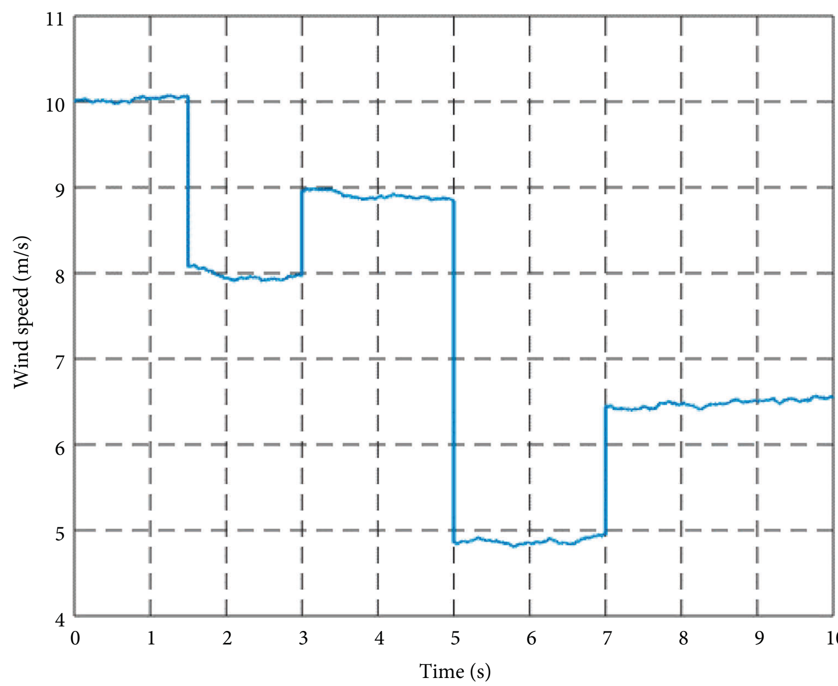

Figure 14: Wind speed profile.

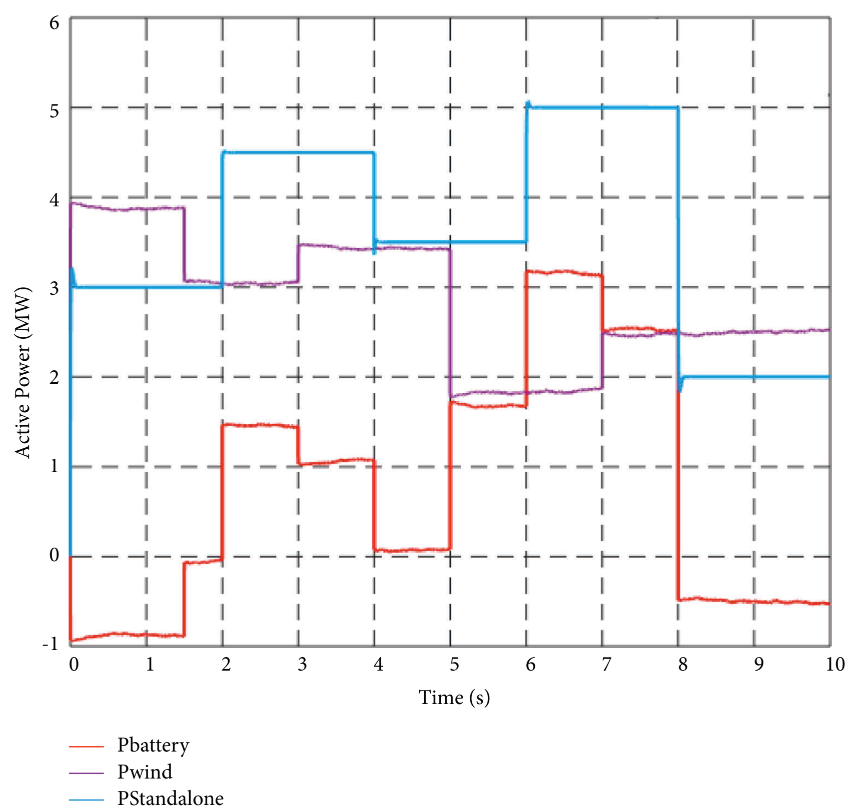

Figure 15: Dynamic response of power for standalone (wind turbine and battery).

Thus, the controller will generate the desired value for the reference of the power of the battery and will manage the power flow into four (04) operating modes as follows:

(i) *Mode 1*. If $dP > 0$ and $SOC_{bat} < SOC_{max}$, surplus power will be charging the battery

(ii) *Mode 2*. If $dP < 0$ and $SOC_{bat} > SOC_{min}$, the battery will be used for the power balance between generation and consumption

(iii) *Mode 3*. When the battery charge reaches its maximum $SOC_{bat} > SOC_{max}$ and $dP > 0$, the wind

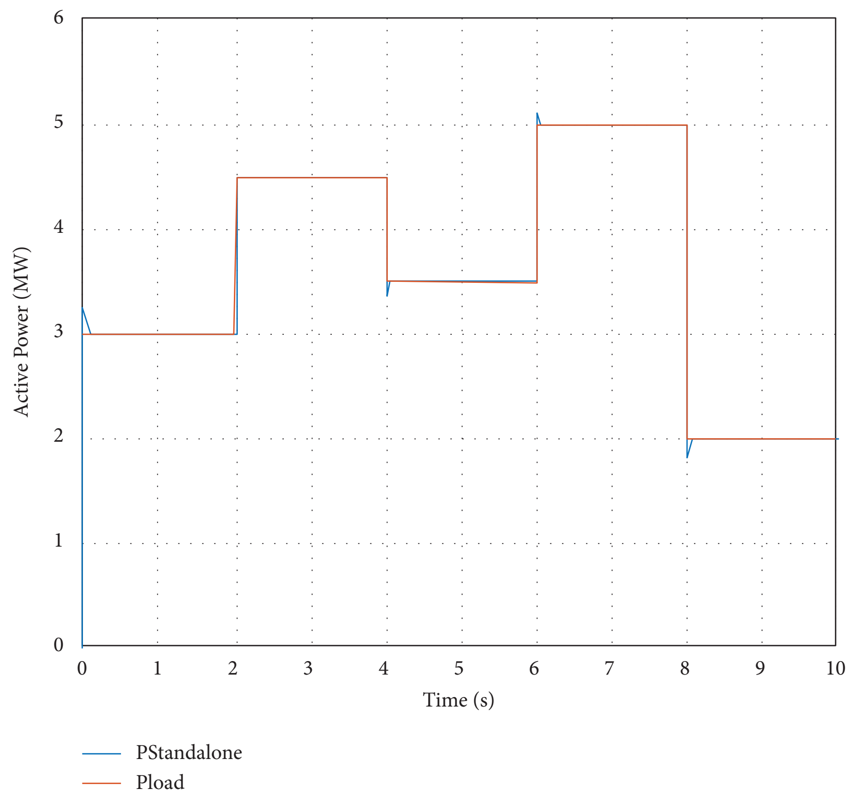

Figure 16: Dynamic performance analysis of the standalone system.

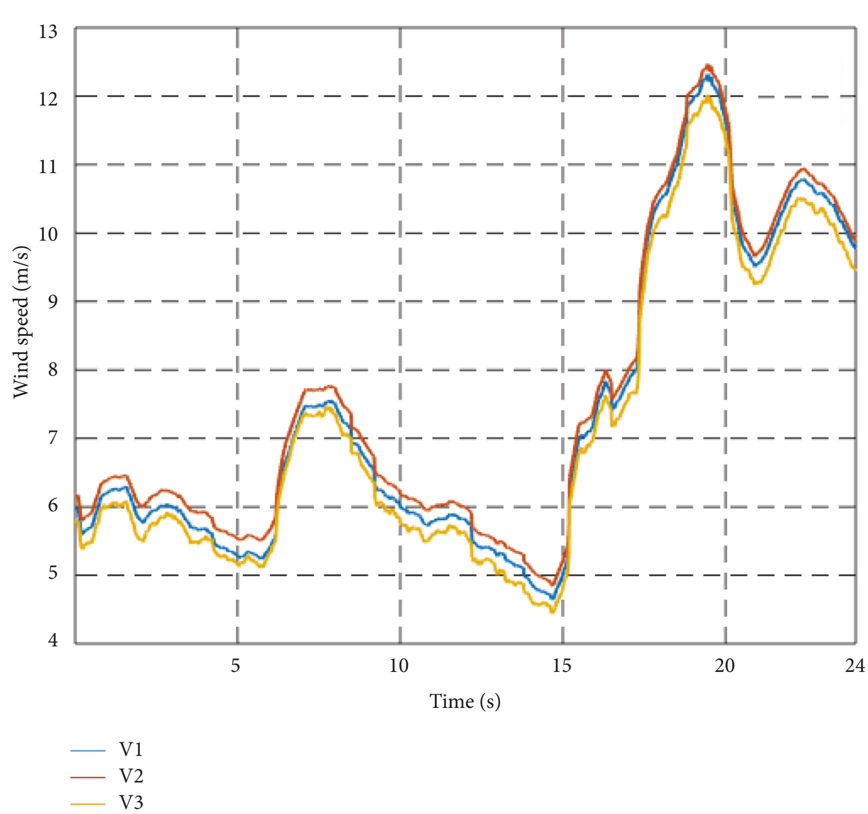

Figure 17: Wind speed profiles.

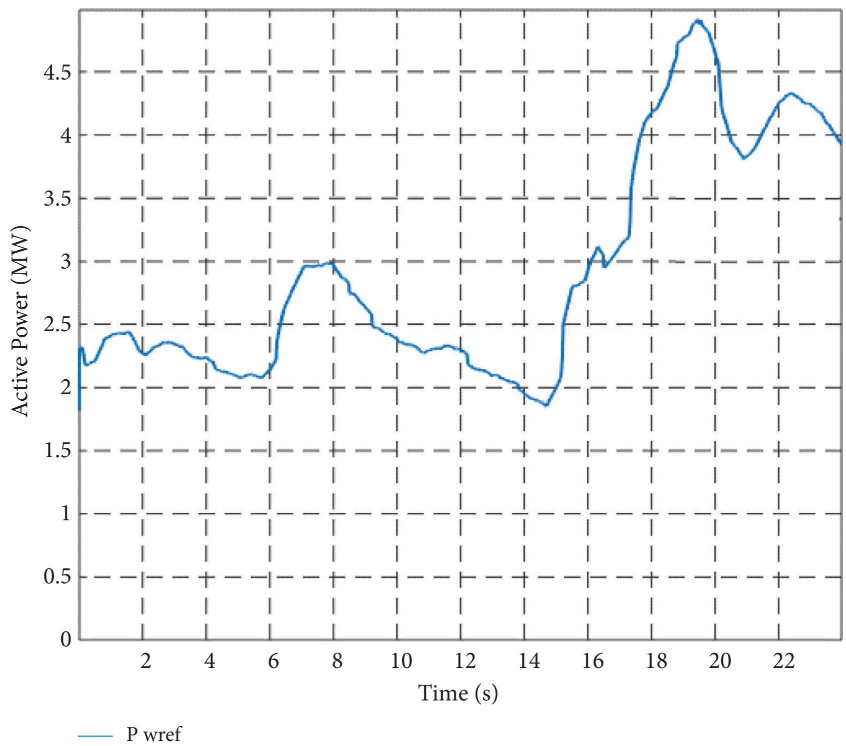

Figure 18: Wind turbine power reference.

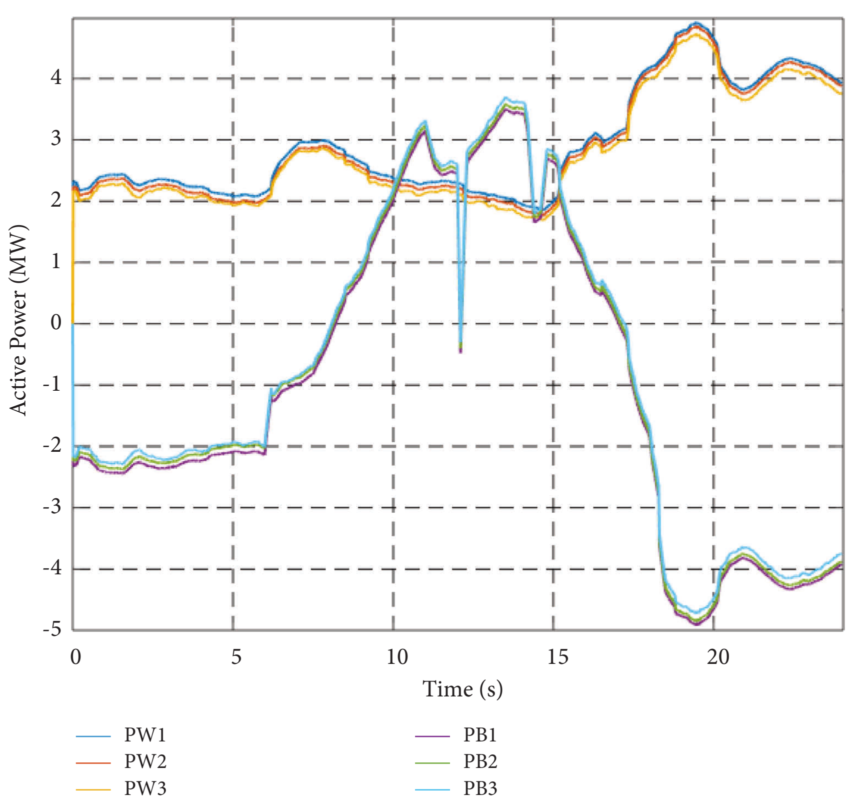

Figure 19: Standalone power for each profile.

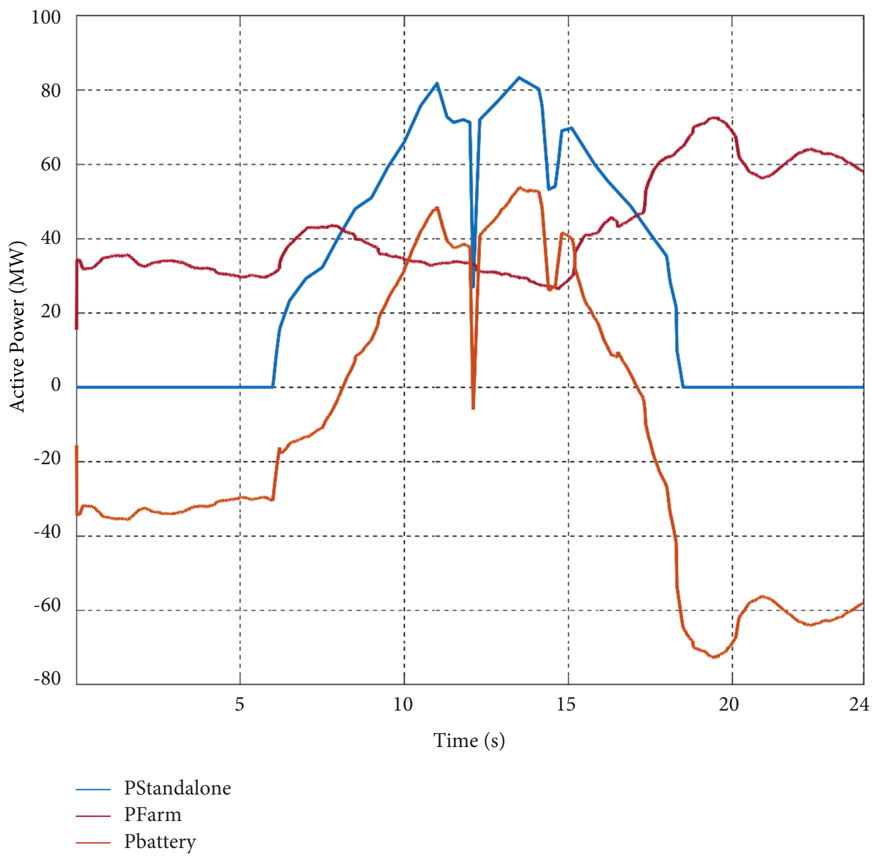

FIGURE 20: Active power output of the wind farm during load and wind speed step changes.

turbine power will be reduced to meet only the load demanded power

(iv) *Mode 4*. If $dP < 0$ and the battery charge reaches its minimum $SOC_{bat} < SOC_{min}$, the controller will disconnect the load and the battery will be charged

Figure 7 shows the flow chart used in this work.

Figures 8–10 show the membership functions used for the input data. Table 1 gives the corresponding rules.

4. Simulation Results

To demonstrate the effectiveness of the proposed control strategy, various sets of simulation case studies under various scenarios have been done and reported below.

4.1. Control of Individual DFIG Wind Turbine. Figure 11 shows the wind speed profile response.

Figure 12 shows the stator active power and its reference profile using PI and SOMC, whereas Figure 13 shows the stator reactive power and its reference profile using PI and SOMC.

It can be seen from Figures 11, 12, and 13 that the proposed SOSMC controller has a quicker response than the traditional PI controller and tracks almost perfectly the references. Furthermore, we observe that the dynamic performance of the powers under the SOMC control is fast and robust. It has also smooth control signals leading to a quasi elimination of the chattering phenomenon.

The simulation results indicate that the SOSMC forces the system states to converge to their desired values instantly which make it appealing for wind energy for stability and power quality at varying wind speeds.

Moreover, the reactive power is kept to zero which may allow the power factor to be close to unity.

4.2. Power Management Strategy. To evaluate the designed power management, Figure 14 is included to show the wind speed changes.

Wind turbine power tracks the MPPT reference and provides power to satisfy the load, whereas the backup storage is used for power balance and the battery converter will monitor the direction of flow.

In Figure 15, the power-sharing of the wind turbine and the battery bank are shown.

The battery storage system will be used to synchronize the power flow between the turbine power and the load. Thus, from the results shown, we can see that the proposed strategy successfully manages the control of the output power at a constant value.

Usually, the wind speed may change quickly leading to oscillations that may affect the load; fortunately with the proposed method along with the battery bank, the change of wind power is effectively compensated.

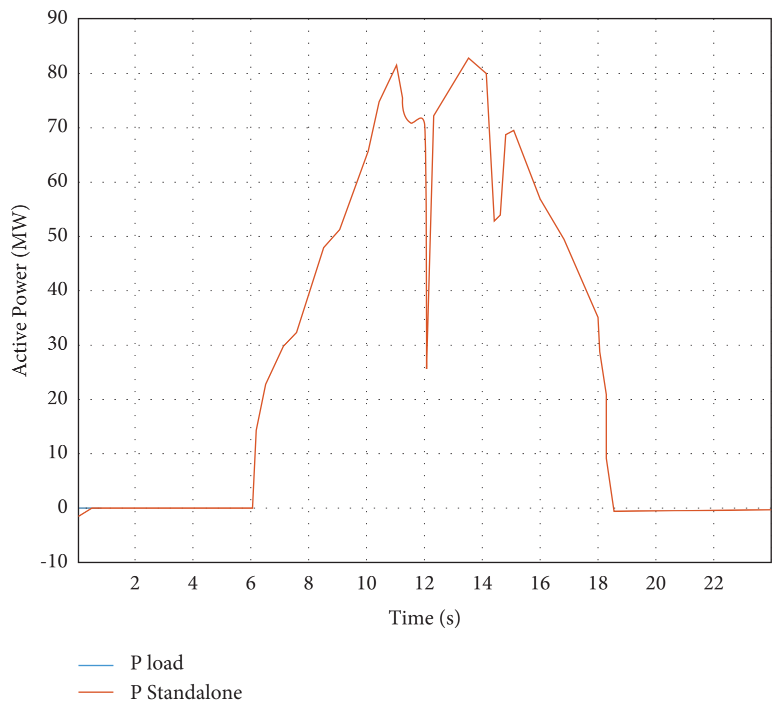

Figure 21: Performance of the wind farm power during load and wind speed step changes.

Figure 15 shows the effective battery response to the decline of wind power with slow wind speed. This may prove that the proposed method is capable of quickly and precisely controlling the battery to balance the power.

Figure 16 demonstrates again the effectiveness of the power balance under different generation scenarios and external variations.

4.3. Wind Farm Supervisory Control. Figure 17 shows the wind speed profiles of three wind turbines composed of 15 turbines. It shows that the wind speeds vary around their mean values at a range of ±0.4 m/s.

Figure 18 shows the reference of the wind power generated by the supervisory system according to the power demand. The energy storage system keeps the system stable for any undesired conditions. These responses show the effectiveness of the battery model in terms of smoothing the fluctuating output power of the aggregated wind farm as shown in Figure 19

Figure 19 shows that it effectively follows the pattern of wind speed since any change in wind power may cause an undesirable frequency change in the system.

Figure 20 shows the necessity of the battery for the power tracking capabilities of the standalone system for active power generation.

It can be observed that when the wind power generated is greater than the power needed by the load, the excess will be transferred to the storage system. However, when the generated power cannot satisfy the needed load power, then the battery will be sought to deliver the required power via the DC bidirectional converter. It can also be seen that the power of the battery changes to maintain the stability of the system.

Finally, Figure 21 is reported to show the power distribution curve where it is noticeable that maximum power can be extracted even in the presence of internal and external uncertainties.

5. Conclusion

In this paper, a coordinated control strategy for hybrid microgrid is proposed. At the local level, a second-order sliding mode control scheme to improve the dynamic performance of a wind turbine has been proposed, which provided a better dynamic response, more robust control, accurate speed adjustment, and less steady-state error. At the system level, since the wind source is not reliable in terms of power quality and sustainability, a power management system is required to ensure a continuous power flow to the load. In this paper, a smart power management system was developed to handle the change effects of the wind speed and amount of the power load.

The proposed power management not only provided the stability of the complete system but also allowed to control effectively the charging and discharging process of the battery leading to its high performance and longevity.

The simulation results reported in this paper have proved that the proposed control technique is efficient in controlling the power flow for all operating sequences and may manage accurately the whole system under different scenarios of power generation while maintaining the state of charge of the battery at an acceptable level.

Data Availability

The data used to support the findings of this study are available from the corresponding author upon request.

Conflicts of Interest

The authors declare that they have no conflicts of interest.

Acknowledgments

This project was funded by the Ministry of Education (MoE) in Saudi Arabia through the Islamic University of Medinah (IUM) under the Institutional Finance Program of the Deanship of Scientific Research (DSR) with a Grant no. 10/20 in 2020. The authors acknowledge with gratitude the support of the MoE and DSR.

References

[1] IRENA, *Towards 100% Renewable Energy: Status, Trends and Lessons Learned*, IRENA, Abu Dhabi, UAE, 2019.

[2] B. Meghni, D. Dib, M. Mordjaou, and A. Saadoun, "Effective supervisory controllers designed for optimal energy management in permanent magnet synchronous generator wind turbine with battery storage," *Wind Engineering*, vol. 40, no. 2, pp. 115–133, 2016.

[3] T. Vigneysh and N. Kumarappan, "Autonomous operation and control of photovoltaic/solid oxide fuel cell/battery energy storage based microgrid using fuzzy logic controller," *International Journal of Hydrogen Energy*, vol. 41, no. 3, pp. 1877–1891, 2016.

[4] B. Meghni, D. Dib, and A. T. Azar, "A second-order sliding mode and fuzzy logic control to optimal energy management in wind turbine with battery storage," *Neural Computing & Applications*, vol. 28, no. 6, pp. 1417–1434, 2017.

[5] I. Hamdan, A. M. A. Ibrahim, and O. Noureldeen, "Modified STATCOM control strategy for fault ride-through capability enhancement of grid-connected PV/wind hybrid power system during voltage sag," *SN Applied Sciences*, vol. 2, no. 3, pp. 364–419, 2020.

[6] A. Bensaber, M. Benghanem, A. Guerouad, and M. Amar Bensaber, "Power flow control and management of a hybrid power system," *Przeglad Elektrotechniczny*, vol. 1, no. 1, pp. 188–192, 2019.

[7] T. Ouyang, A. Kusiak, and Y. He, "Modeling wind-turbine power curve: a data partitioning and mining approach," *Renewable Energy*, vol. 102, pp. 1–8, 2017.

[8] R. Hemmati, "Technical and economic analysis of home energy management system incorporating small-scale wind turbine and battery energy storage system," *Journal of Cleaner Production*, vol. 159, pp. 106–118, 2017.

[9] B. Yang, T. Yu, H. Shu, J. Dong, and L. Jiang, "Robust sliding-mode control of wind energy conversion systems for optimal power extraction via nonlinear perturbation observers," *Applied Energy*, vol. 210, pp. 711–723, 2018.

[10] M. Baharizadeh, H. R. Karshenas, and J. M. Guerrero, "An improved power control strategy for hybrid ac-dc microgrids," *International Journal of Electrical Power & Energy Systems*, vol. 95, pp. 364–373, 2018.

[11] P. K. Dash, R. K. Patnaik, and S. P. Mishra, "Adaptive fractional integral terminal sliding mode power control of UPFC in DFIG wind farm penetrated multimachine power system," *Protection and Control of Modern Power Systems*, vol. 3, no. 1, p. 8, 2018.

[12] B. Meghni, D. Dib, A. T. Azar, and A. Saadoun, "Effective supervisory controller to extend optimal energy management in hybrid wind turbine under energy and reliability constraints," *International Journal of Dynamics and Control*, vol. 6, no. 1, pp. 369–383, 2018.

[13] L. Xu and P. Cartwright, "Direct Active and Reactive Power Control of DFIG for Wind Energy Generation," *IEEE Transactions on Energy Conversion*, vol. 21.

[14] O. Noureldeen and I. Hamdan, "A novel controllable crowbar based on fault type protection technique for DFIG wind energy conversion system using adaptive neuro-fuzzy inference system," *Protection and Control of Modern Power Systems*, vol. 3, no. 1, pp. 35–12, 2018.

[15] M. Guo, D. Sun, and B. T. He, "Direct Power Control for Wind-Turbine Driven DFIG with Constant Switch Frequency," in *Proceedings of the ICEMS*, Seoul, Republic of Korea, October 2007.

[16] F. K. A. L. Luna, P. Rodriguez, E. H. Watanabe, and R. Teodorescu, "Comparison of Power Control Strategies for DFIG Wind Turbines," in *Proceedings of the 2008 34th Annual Conference of IEEE Industrial Electronics*, Orlando, FL, USA, November 2008.

[17] AG. Abo-Khalil and G. Ahmed, "Synchronization of DFIG Output Voltage to Utility Grid in Wind Power System," *Renewable Energy*, vol. 44, 2012.

[18] G. Abad, J. Lopez, M. Rodriguez, L. Marroyo, and G. Iwanski, *Doubly fed induction machine: modeling and control for wind energy generation*, WIley, Hoboken, NJ, USA.

[19] L. Xu and P. Cartwright, *Direct Active and Reactive Power Control of DFIG for Wind Energy Generation*, vol. 30, no. 1, pp. 257–263, 2006.

[20] A. Miloudi, E.-A. Al Radadi, A. Draou, and Y. Miloud, "Simulation and Modelling of a Variable Gain PI Controller for Speed Control of a Direct Torque Neuro Fuzzy Controlled Induction Machine Drive," in *Proceedings of the 2004 IEEE 35th Annual Power Electronics Specialists Conference (IEEE Cat. No.04CH37551)*, Aachen, Germany, June 2004.

[21] M. J. Morshed and A. Fekih, "Design of a second order sliding mode approach for DFIG-based wind energy systems," in *Proceedings of the 2017 American Control Conference (ACC). 2017*, IEEE, Seattle, WA, USA, May 2017.

[22] D. Sun, X. Wang, H. Nian, and Z. Q. Zhu, "A sliding-mode direct power control strategy for DFIG under both balanced and unbalanced grid conditions using extended active power," *IEEE Transactions on Power Electronics*, vol. 33, no. 2, pp. 1313–1322, 2018.

[23] J. Lopez, P. Sanchis, X. Roboam, and L. Marroyo, "Dynamic behavior of the doubly fed induction generator during three-phase voltage dips," *IEEE Transactions on Energy Conversion*, vol. 22, no. 3, pp. 709–717, 2007.

[24] G. Abad et al., "Direct control of the doubly fed induction machine," in *Doubly Fed Induction Machine*, pp. 363–477, John Wiley & Sons, 2011.

[25] S. E. Aimani, "Modélisation des différentes technologies d'éoliennes intégrées dans un réseau de moyenne tension," Docteur , Docteur2004.

[26] F. Poitiers, *ETUDE ET COMMANDE DE GENERATRICES ASYNCHRONES POUR L'UTILISATION DE L'ENERGIE EOLIENNE - Machine asynchrone à cage autonome - Machine asynchrone à double alimentation reliée au réseau*, Université de Nantes, Nantes, France, 2003.

[27] I E C, *Electrical Simulation Models—Wind Turbines*, International Electrotechnical Commission, Geneva, Switzerland, 2013.

[28] A. Mohammadi, M. H. Ahmadi, M. Bidi, F. Joda, A. Valero, and S. Uson, "Exergy analysis of a Combined Cooling, Heating and Power system integrated with wind turbine and

compressed air energy storage system," *Energy Conversion and Management*, vol. 131, pp. 69–78, 2017.

[29] L. Xu and P. Cartwright, "Direct active and reactive power control of DFIG for wind energy generation," *IEEE Transactions on Energy Conversion*, vol. 21, no. 3, pp. 750–758, 2006.

[30] M. I. Mosaad, A. Abu-Siada, M. M. Ismaiel, H. Albalawi, and A Fahmy, "Enhancing the fault ride-through capability of a DFIG-WECS using a high-temperature superconducting coil," *Energies*, vol. 14, no. 19, p. 6319, 2021.

[31] O. Noureldeen, I. Hamdan, and B. Hassanin, "Design of advanced artificial intelligence protection technique based on low voltage ride-through grid code for large-scale wind farm generators: a case study in Egypt," *SN Applied Sciences*, vol. 1, no. 6, pp. 515–519, 2019.

[32] S. AlGhamdi, I. Hamdan, and M. M. M. Youssef & Omar Noureldeen, "Development and Application of Fuzzy Proportional-Integral Control Scheme in Pitch Angle Compensation Loop for Wind Turbines," *Machines*, vol. 9, 2021.

[33] D. W. Zhi, L. Xu, and J. Morrow, "Improved Direct Power Control of Doubly Fed Induction Generator Based Wind Energy System," in *Proceedings of the IEMDC*, Antalya, Turkey, May 2007.